

Effect of Red-Blue Composite Laser Welding Joint on Microstructure and Properties of Copper Alloy

Hai Cai, Jiahao Zhou, Shuming Zhang, and Panpan Jia*

University of Shanghai for Science and Technology, Shanghai 200093, China

*15051931929@163.com

Abstract

The 3 mm copper was lapped and welded by red-blue laser composite welding, and the near infrared light and blue light were combined by double light source laser welding system. The forming quality and influence mechanism of welded joint after adding blue light were studied. The microstructure and mechanical properties of the welded joint are analyzed. The results show that the absorption rate of near infrared light of copper alloy is greatly increased and the welding stability is improved after adding blue light. With the increase of blue light power, the weld surface is smooth and the weld penetration depth and width increase. Under the effect of blue light insulation, the grain growth time of weld structure is prolonged; Moreover, after adding blue light, the stability of molten pool is increased, and the microstructure composition of weld is homogenized, so the hardness value of weld zone tends to be stable, and the optimal value of blue light power is 800 W. The tensile test results show that the tensile strength and plasticity of the joint increase with the increase of blue light power. When the blue light power is 800W, the maximum tensile strength is 273.8 MPa and the elongation is 7.33%.

Keywords

Laser Welding; Copper Alloy; Blue Light; Microstructure; Mechanical Property.

1. Introduction

Copper and its alloys are widely used in the fields of petroleum, chemical industry, marine communication, and power systems due to their excellent electrical conductivity, thermal conductivity, corrosion resistance, and mechanical properties[1]. However, due to the high cost of copper alloys, weight reduction and volume optimization have become important research directions in the application of copper alloys[2]. In the field of new energy vehicles, copper alloys are used in many critical components, ranging from cooling systems, electric braking systems, to hydraulic systems. With the increasing application of copper alloys in new energy vehicles, the importance of welding technology is becoming increasingly prominent[3].

The high thermal conductivity of copper and its alloys has always been a major challenge in the welding process. Traditional manual arc welding and manual argon arc welding methods are difficult to achieve ideal welding results due to insufficient power density [4][5]. Laser welding has become an ideal choice for copper alloy connection processes due to its characteristics of rapid heating, rapid cooling, high laser power, narrow heat-affected zone, and high-speed welding[6]. Currently, the mainstream laser welding mainly uses near-infrared lasers with wavelengths between 760nm and 1mm. However, the reflectivity of copper alloys to this type of light is as high as 95%, resulting in extremely low energy utilization efficiency in near-infrared laser welding of copper. To improve the laser weldability of copper alloys, scholars have conducted extensive research on surface treatment

of copper alloys, such as oxidation treatment [7][8] and blackening treatment[9] on the surface of copper, to increase the absorption of laser power by copper. Although this method can improve the weldability of copper, it increases the production process and significantly raises the production cost. Therefore, researchers have begun to explore the application of visible light lasers in the short-wave band (300-600nm) in copper welding[10]. The absorption rate of copper alloys to short-wave blue light with a wavelength of 450nm is as high as 65% [11], which provides a new possibility for the welding of copper alloys. Hummel et al.[12] used a 150W blue semiconductor laser to perform laser welding on thin copper alloy sheets and studied the influence of welding parameters on the joint. Britten et al. [13] achieved heat conduction welding of copper using a 1kW blue laser, achieving repeatable and uniform welds. The use of higher-power blue light can achieve keyhole welding of copper alloys. By adopting short-wave light sources, the energy utilization efficiency of copper alloy welding can be effectively improved, thereby obtaining better welding results.

In this paper, T2 copper is selected for red-blue laser hybrid welding, and the effects of adding blue light on the weld microstructure and mechanical properties are studied. Furthermore, the mechanism of the influence of hybrid light sources on the forming quality of T2 copper laser welded joints is analyzed.

2. Organization of the Text Experimental Procedure

2.1 Test Materials and Equipment

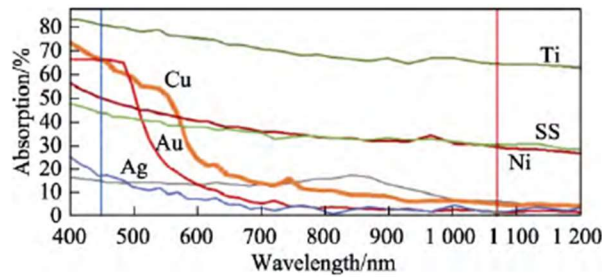
The test selects T2 copper plate with specifications of 100mm×50mm×3mm. The microstructure of T2 copper base metal is shown in Fig. 1, and the chemical composition is shown in Table 1. The absorption curve of T2 copper for different wavelength lights is shown in Fig. 2(a) (from the research of Zediker et al. [14]). The absorption rate of T2 copper for light with a wavelength of 1070 nm is about 4%, and the absorption rate for light with a wavelength of 450 nm is about 65%. Fig. 2(b) shows the absorption rate and thermal conductivity of T2 copper for 1070μm laser varying with temperature (from the research of Wenmin et al. [15]). It can be seen that the absorption rate of T2 copper for 1070 μm laser increases with the increase of temperature, rises significantly near the melting point, and gradually stabilizes.

Table 1. Chemical Composition of T2 Purple Copper

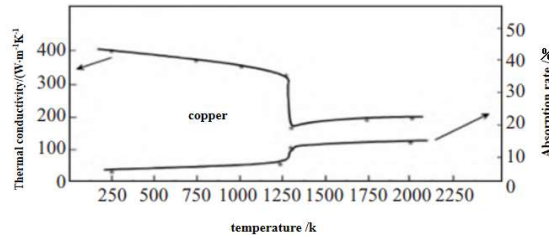
material	P	Bi	Fe	Pb	S	Cu
Ingredients	0.001%	0.001%	0.005%	0.005%	0.005%	99.983%



Fig. 1 Microstructure of parent metal



(a) Absorption curve of copper for light of different wavelengths[14]



(b) Temperature dependence of absorption rate and thermal conductivity of copper for 1070µm laser[15]

Fig. 2 diagram of absorption rate change of red copper

The schematic diagram of the dual-light-source hybrid laser welding equipment is shown in Fig. 3. It adopts a 2000W rated power Feibo near-infrared fiber laser and an 800W rated power hard science research institute blue light semiconductor laser; a BW290 dual-band hybrid welding laser head produced by Scansonic; and a KUKA KR210 robot. The laser spot is circular with a fiber core diameter of 100 µm. 99.99% pure argon is used as the protective gas with a flow rate of 20 L/min. The test plate adopts a lap overlay welding form. The welding speed, laser power, and other process parameters are shown in Table 2.

Table 2. Composite Light Source Laser Welding Process Parameters

variable	P_{blue}	P_{red}	V_w	Defocus amount	Protective gas flow rate	Spot shape
parameter	0; 400-800W $\Delta=200$ W	2800W	20mm/s	0	20L/min	rotundity

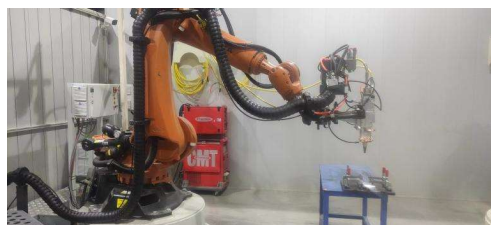


Fig 3 Double light source composite laser welding equipment

2.2 Analysis of Microstructure and Mechanical Properties of Joints

A 15 mm x 10 mm sample of the weld cross-section was cut using a wire cutting machine. The sample was polished to a mirror finish using metallographic abrasive paper and polishing agent before being placed in an anhydrous ethanol solution for ultrasonic cleaning. A corrosive agent was prepared using 3g of ferric chloride, 2mL of hydrochloric acid, and 96mL of anhydrous ethanol for metallographic corrosion. The microstructure of the weld area was observed using a VHX-500F KEYENCE digital

metallographic microscope. The welded joint was analyzed using a Merlin compact SEM scanning electron microscope with an acceleration voltage of 20kV.

The Vickers hardness test was conducted on the welded joint using a DHV-1000Z microhardness tester with a loading load of 100g and a holding time of 10s. The interval between test points was 0.5mm. The micro Vickers hardness distribution and characteristics of each area of the welded joint were analyzed. Tensile specimens were cut along the direction perpendicular to the weld seam, with the preparation referencing the GBT228.1-2010 standard. Tensile tests of the welded joint were conducted on a Zwick/Roell Z050 universal tensile testing machine with a maximum pressure of 2 MPa, a power of 1.1 kW, a tensile speed of 1 mm/min, and a maximum test force of 50 kN. After tensile failure, the fracture morphology was observed under a scanning electron microscope to analyze the characteristics of the tensile fractures in different parts of the welded joint. The dimensions of the tensile specimens are shown in Fig. 4 below:

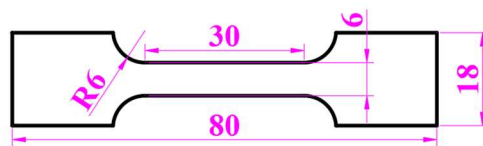



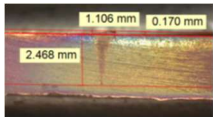

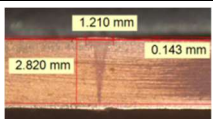

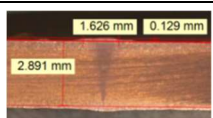
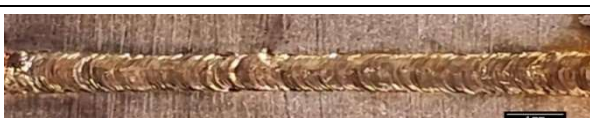
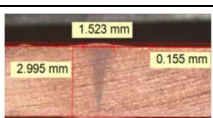
Fig. 4 Schematic diagram of tensile specimen size

3. Results and Discussion

3.1 Surface Quality of Weld Seam

Table 3 shows the macro morphology of the weld. It can be seen that without the addition of blue light, the weld surface exhibits significant defects such as porosity and splashing, and this appearance cannot meet the actual production requirements. With the addition of blue light, the weld surface becomes smoother, and the weld formation is good, without defects such as undercutting, porosity, and splashing. As shown in Fig. 5, both the penetration depth and width of the weld, as well as the width in the middle of the weld, increase. The cross-sectional profile transforms from a "nail-like" shape to a "V-shaped" profile. This is because the addition of blue light increases the temperature of the copper plate, thereby enhancing the absorption rate of copper for near-infrared light. The laser energy reflected by the copper decreases, and more laser energy is used to melt the base material, resulting in increased penetration depth and width of the weld.

Table 3. Surface morphology and cross-section of welds under different power blue light conditions

Blue light power(W)	Surface morphology of weld seam	Cross section of weld seam
0		
400		
600		
800		

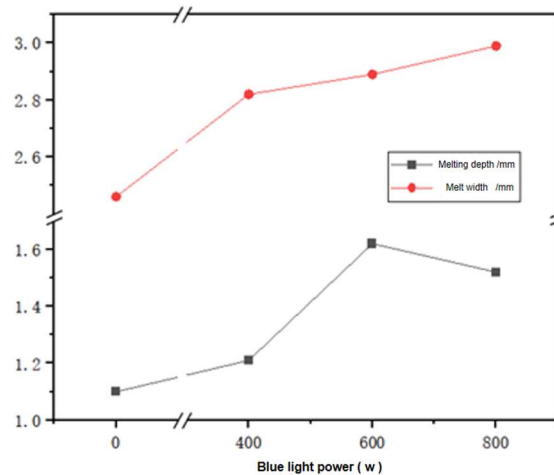


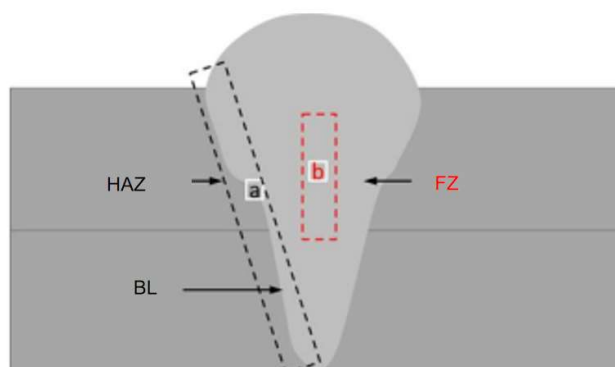
Fig. 5 Distribution of average weld penetration and weld width under different blue light powers

3.2 Microstructure of Welded Joints

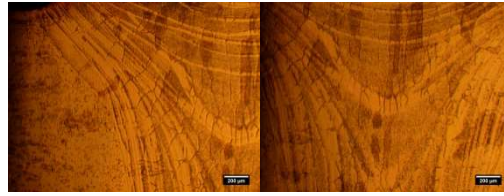
As can be seen from the weld cross-sectional morphology shown in Table 3, the red-blue hybrid laser welding has achieved good welding results, with a full weld and no internal defects such as porosity or cracks. Metallographic analysis was performed on the weld joint, and two locations were selected for analysis of the weld structure in Fig. 6(a), namely the heat-affected zone (HAZ) and the center of the weld. From Figs 6(b), (c), (d), and (e), it can be concluded that the grain structure in the HAZ is coarse due to the influence of the welding heat cycle, and the microstructure near the fusion line grows as columnar crystals perpendicular to the center of the weld along the temperature gradient. The microstructure in the center of the weld is typically equiaxed grain structure. The equiaxed grains in the center of the weld are refined and have uniform grain sizes.

When using a single near-infrared laser welding, due to the high laser power and relatively large temperature gradient, the cooling rate of the weld is fast, and the microstructure in the fusion zone is fine cellular grain structure, forming smaller-sized equiaxed grains in the center of the weld, as shown in Fig. 6(b).

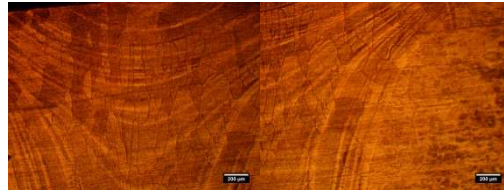
When adding a blue light semiconductor laser and a near-infrared fiber laser for hybrid welding, the blue light preheats the copper plate, thereby increasing the absorption rate of copper for near-infrared light[16]. During the welding process, the temperature inside the molten pool is higher, and the microstructure in the fusion zone transforms into coarse α -Cu structure, as shown in Figs 6(c-e). Due to the coaxial welding with dual light sources, the weld area is thermally insulated by the blue light, resulting in the same temperature gradient in all directions of the weld center, slower cooling speed, longer grain growth time in the center area, and larger grain sizes of the equiaxed grain structure. The increase in grain size is beneficial for improving mechanical properties.



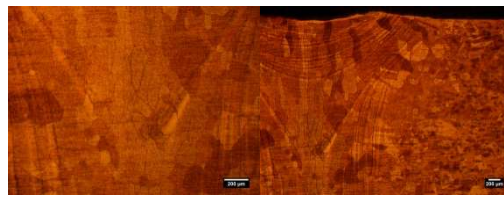
(a) Schematic diagram of each area in the cross-section of the weld seam



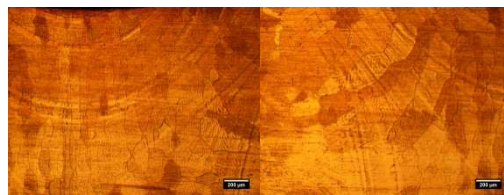
(b) 0W blue light heat affected zone and center structure of weld seam



(c) 400W blue light heat affected zone and center structure of weld seam



(d) 600W blue light heat affected zone and center structure of weld seam



(e) 800W blue light heat affected zone and center structure of weld seam

Fig. 6 Microstructure of weld heat affected zone and weld center under different power blue light.

3.3 Microhardness of Welded Joints

Microhardness measurements were performed on the weld joint as shown in Fig. 7, and the results are presented in Fig. 8.

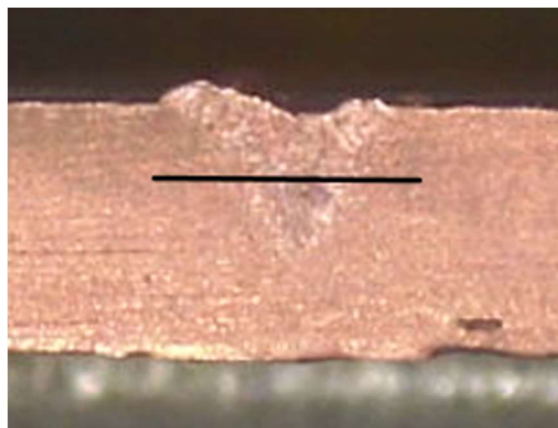


Fig. 7 schematic diagram of microhardness measurement

Fig. 8 shows the microhardness distribution of the welded joint, with the hardness distribution curve presenting a "W" shape. The hardness value is highest in the base metal area, while it is significantly lower in the weld center and heat-affected zone compared to the base metal. The maximum microhardness value at the welded joint appears in the weld center region, then suddenly decreases in the heat-affected zone, with the lowest value being about 62% of the base metal, indicating

softening of the welded joint. When welding without blue light, the equiaxed grain structure in the weld center has the smallest grain size and the highest hardness value, with a more significant decrease in hardness in the heat-affected zone. When using a blue light semiconductor laser and a near-infrared fiber laser for hybrid welding, as the blue light power increases, the grain size of the equiaxed grain structure in the weld center gradually increases, and the hardness value gradually decreases. The change in hardness in the heat-affected zone is not as significant as when blue light is not used. This indicates that the microhardness decreases as the grain size increases.

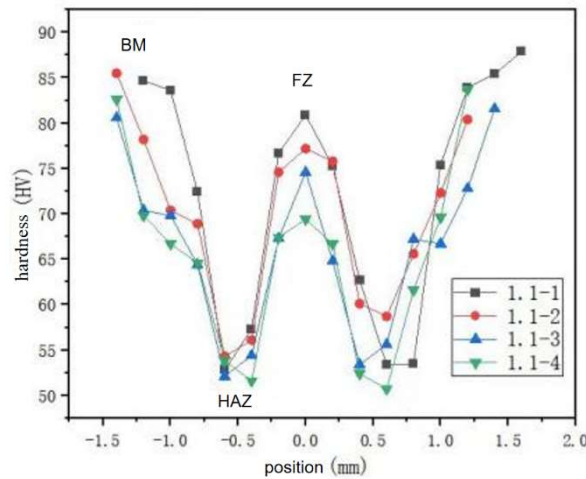


Fig. 8 microhardness distribution of welded joints

3.4 Tensile Performance of Welded Joints

According to the sampling method shown in Fig. 3, three tensile specimens were taken from welding parts with various parameters for tensile testing. The results are shown in Table 4 and Fig. 9. When blue light is added for hybrid welding, the tensile properties of the welded joint gradually increase, with both tensile strength and elongation increasing. When the blue light power reaches 800W, the tensile strength of the welded joint reaches a maximum of 273.8 MPa, and the elongation is 7.33%, which is 46 MPa higher than that of welding parts without blue light. Cross-sectional analysis of the fractured specimens is shown in Fig. 9, indicating that the fracture locations of the welded joints are all located in the heat-affected zone, and the plasticity of the welded joints is enhanced with the addition of blue light.

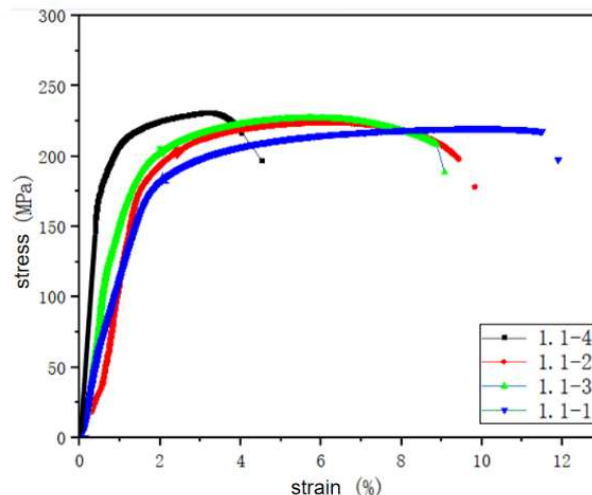
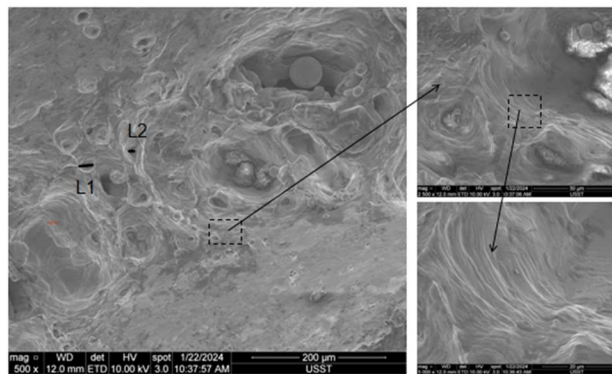


Fig. 9 tensile true stress-strain curves of welded joints under different blue light power

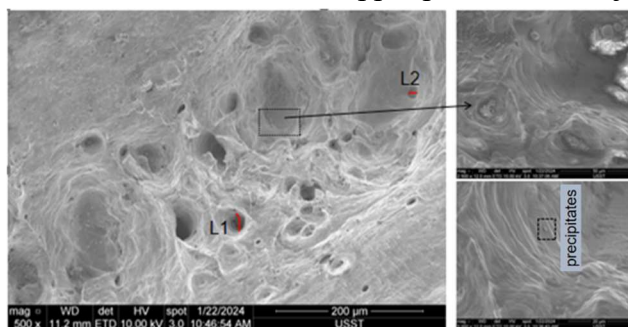
Table 4. Tensile strength and elongation of welded joints under different blue light power

Blue light power(P/W)	tensile strength(Rm/MPa)	Elongation rate(A/%)
0	227.4	5.66
400	231.3	5.97
600	252.7	6.52
800	273.8	7.33

After tensile fracture of the welded joint using a single near-infrared laser welding, the joint exhibited significant plastic deformation. SEM analysis of the fractured welding joint is shown in Figure 10. There are obvious dimples at the fracture site of the welded joint. The dimples at the upper part of the weld are large and shallow, with shallow tear ridges and varying sizes of dimples. The shallow dimples are approximately 14 μm in size, while the smaller dimples are around 6 μm in size, as shown in Fig. 10(a). The average size of the deeper dimples is approximately 10 μm . The dimples at the bottom of the joint are finer and more equiaxed, as shown in Fig. 10(b), and are significantly deeper than those at the upper part of the weld pool. The larger dimples are approximately 9 μm in size, while the smaller dimples are around 3 μm in size, indicating good plasticity.



(a) Morphology of tensile fracture surface on the upper part of welded joint under 0W blue light



(b) Tensile fracture morphology of the lower part of the welded joint under 0W blue light

Fig. 10 Fracture morphology of welded joint under 800w blue light

4. Conclusion

This paper studies the impact of red and blue laser hybrid welding on the microstructure and properties of copper alloy welded joints, analyzing the high absorption rate of copper alloy to blue light and the influence mechanism of changes in thermal conductivity after preheating of copper alloy on the forming quality of welded joints. The conclusions are as follows:

1) After adding blue light, the temperature reaches the melting point under the action of blue light, and the absorption rate of copper alloy to near-infrared light is significantly increased at this time.

Stable welding can be achieved using lower-power near-infrared light. As the blue light power gradually increases, both the depth and width of the weld increase, and the cross-sectional profile changes from a "nail shape" to a "V shape". The weld surface tends to be smooth, and the weld formation is good without defects such as undercutting, pores, and spatter.

2) With the increase of blue light power, the grains in the center of the weld grow larger, and the hardness value tends to be stable. Due to the heat preservation effect of blue light, the grain size is larger, and the hardness value in the weld zone of the joint decreases, resulting in joint softening.

3) The tensile strength of the welded joint increases with the increase of blue light power. When the blue light power is 800 W, the tensile strength is the highest at 273.8 MPa, and the elongation is 7.33%. Observing the morphology of the tensile fracture through SEM, it is found that the fracture without blue light is mainly composed of coarse dimple structure with shallow depth. The tensile fracture position of the joint is in the center of the weld of the joint. After adding blue light, the fracture has a uniform and deep distribution of dimples with obvious tear ridges. When the blue light power is 800 W, the forming quality of the welded joint is the best.

References

- [1] Wang, J, Chu, C, Gu, J, et al. Simulation Analysis of Temperature Field in Laser Welding of Clutch Inner Plate Bracket. *Mechanical Design and Manufacturing*, 2020(07),101-104.
- [2] Tang, S, Du, Y, Wang, J, et al. Progress in the Study of Aluminum-copper Laser Welding in New Energy Power Batteries. *Nonferrous Metal Processing*, 2024, 53(01), 16-22.
- [3] Sun, J. Study on Laser Welding Process and Application of Purple Copper. Wuhan: Wuhan University of Technology, 2015.
- [4] Tianyu X ,Libo W ,Xiuquan M , et al.Solidification sequence and crystal growth during laser welding stainless steel to copper[J].*Materials Design*,2023,225.
- [5] Suman C ,N. L T ,Dongkyoung L .Mechanical and microstructural investigation of dissimilar joints of Al-Cu and Cu-Al metals using nanosecond laser[J].*Journal of Mechanical Science and Technology*,2022, 36(8):4205-4211.
- [6] Biro E, Weckman D C, Zhou Y. Pulsed Nd:YAG laser welding of copper using oxygenated assist gases [J]. *Metallurgical & Materials Transactions A*, 2002, 33 (7):2019-2030.
- [7] Moalem A,Witzendorff P V, Stute U,et al.Reliable copper spot welding with IR laser radiation through short prepulsing [J].*Procedia CIRP*,2012,3(1):459-464.
- [8] Dacian I ,GilbertRainer G ,ZenoIosif P , et al.Determination of proper parameters for ultrasonic welding of copper plate with copper wire strands[J].*Vibroengineering Procedia*,2023,51167-172.
- [9] Sairam C ,Balaji G S ,Menon A A , et al.Experimental Investigation on TIG Welded Copper B370 and Stainless Steel 434[J].*International Journal of Vehicle Structures Systems*,2023,15(6):829-832.
- [10] Y.D. W ,P. X ,F.C. L , et al.Influence of processing innovations on joint strength improvements in friction stir welded high strength copper alloys[J].*Materials Science Engineering A*,2023,872.
- [11] Geng H ,Xu G ,Liu J , et al.Rotary friction welding of pure aluminum to preheated brass[J].*Welding in the World*,2022,66(11):2371-2376.
- [12] Hummel M ,Schöler C ,Häusler A , et al.New approaches on laser micro welding of copper by using a laser beam source with a wavelength of 450 nm[J].*Journal of Advanced Joining Processes*,2020,1(C).
- [13] Britten S,Krause V.Industrial blue diode laser breaks 1 kW barrier[J].*Photonics Views*,2019,16(2):30-33.
- [14] M.S.Zediker,R.D.Fritz,M.J.Finuf,J.M.Pelaprat,Laser welding components for electric vehicles with a high-power blue laser system,[J].*Laser Appl*.32(2)(2020),022038.
- [15] Wenmin T ,Yongming H ,Xianhuan W , et al.An investigation on microstructure and mechanical properties of H62 brass thin-sheet by fiber laser welding: Experiments and multi-scale simulations[J]. *Optics and Laser Technology*,2024,171110376-.
- [16] Y. Ishige, H. Hashimoto, N. Hayamizu, N. Matsumoto, F. Nishino, M. Kaneko, H. Nasu, G. Gajdatsy, A. Cserteg, K. Jahn, T. Hirao, H. Matsuo, R. Konishi, M.S. Zediker, Blue laser-assisted kW-class CW NIR fiber laser system for high-quality copper welding *SPIE LASE 2021 16680M*.